Universität Freiburg
Advanced Physics Lab Course
FP1 2024-2

Experiment 3
Superconductivity

Full Scientific Report

[redacted]

October 1, 2024

Lab Work conducted: September 26 & 27

Assistant: [redacted]

Contents

Analysing the Resistivity Behaviour of Superconductor $YBa_2Cu_3O_{7-x}$ and Normal Conductor Cu as a Function of Temperature

Abstract

Superconductors are materials which, under the right conditions, exhibit a sudden loss of their electrical resistivity below a certain critical temperature T_c, along with a repulsion and expulsion of magnetic field lines. This has countless applications in science and technology, as it allows for, amongst others, the creation of extremely strong electromagnets, effective energy storage systems and general reduction of energy losses. The goal of this experiment is to analyse and compare the temperature-voltage curves of the high-temperature superconductor $YBa_2Cu_3O_{7-x}$ and of a piece of copper wire down to near -200 °C. Measurements are conducted using the 4-point-probe technique for measuring small resistances and liquid nitrogen is used to cool down the samples. The critical temperature of the superconductor is found to be $T_c = -164(5)$ °C and a linear decrease of voltage is observed for Copper when cooling it down through the same temperature range. Different systematic and statistical uncertainties are be taken into account and some fluctuations and deviations from the expected behaviour are discussed.

1 Introduction

While normal conductors show a continuous decrease in electrical resistivity at decreasing temperature and never reach zero, some materials display an abrupt transition below a certain temperature, where the resistivity falls to zero. This effect was first observed in the case of mercury, in 1911 by Kamerlingh Onnes, who then coined the term superconductivity [Dem17]. A theoretical explanation for superconductivity was offered in 1957 by Bardeen, Cooper and Schrieffer [BCS57; Wer12]: At low temperatures, electron-lattice interactions produce correlated electron pairs. In a simplified model, each electron induces a polarisation of the surrounding lattice which will in turn attract other electrons, hence leading to an effective attraction in between electrons. In fact, it is a dynamical polarisation due to the electron's movement, and electrons of opposite momentum will form correlated pairs - the so-called Cooper pairs. Due to their vanishing total momentum, Cooper pairs barely get scattered during collisions with other electrons and ions, which heavily reduces electrical resistivity [Wer12; Dem17]. This is not the only effect occurring in superconductors - the Meissner-Ochsenfeld effect describes that around the same temperature T_C, perfect diamagnetism emerges, meaning that magnetic fields are expulsed from superconductive materials [Wer12] - but the focus of this experiment lies on the resistivity behaviour.

The bond of Cooper pairs is broken when the temperature is high enough that the electrons' thermal kinetic energy exceeds the bond energy. This critical energy is so low that the transition temperature T_C is below 30 K for many elements and compounds [Dem17]. However, in further research, superconducting compounds with a higher T_C up to more than 100 K have been found. Such high-temperature superconductors are especially sought-after for practical application, as cheaper materials like liquid nitrogen can be used to keep them below their critical temperature, in comparison to e.g. liquid helium. This is the case for the superconductor examined in this experiment.

Superconductivity is a very active field of research, which is driven by the countless applications of the advantageous properties of superconductors. One well known example are MRI machines, which require extremely homogeneous magnetic fields of considerable strength, typically between 1.5 and 3.0 T [MVG23], which can be achieved using superconducting electromagnets. MRI is a non-invasive medical imaging technique, based on the resonance behaviour of proton spins. For the same reason of neading extremely high magnetic field strengths, superconducting magnets are a vital part of most large particle accelerator systems, like the LHC at CERN [CER].
Another example are MagLev technologies, i.e. vehicles floating over rails without rolling friction and at extremely high speeds, making use of strong (superconducting) magnets. There are two main types of maglev systems [Bos24]: electromagnetic suspension (EMS), which is based on the attraction between magnets on both the train and the railway, and electrodynamic suspension (EDS), in which superconducting magnets of the rails repel the magnets on the trains underside. Maglev technologies have a low energy consumption and offer many other advantages like a low noise level and no air pollution, in comparison to many other modes of transportation.
Even within the field of sustainable energy research, superconductivity has become a much discussed concept. Superconducting magnetic energy storage (SMES) is based on the idea that a

current will persist within a superconducting material, even after the originally applied electric field is turned off [AOA22]. Such storage systems can easily be charged and discharged repeatedly and quickly and can contribute, amongst others, to stabilising the electricity grid.

The aim of this experiment is to analyse the behaviour of a superconductor ($YBa_2Cu_3O_{7-x}$) and a normal conductor (Cu) when cooling them down to very low temperatures. We use the four-point-probe technique for measuring resistances and liquid nitrogen to cool down the probes. Additionally, calibrations for the temperature sensors are conducted. Based on the obtained data we will compare the temperature-voltage-curves of the two samples and determine the critical temperature T_c of $YBa_2Cu_3O_{7-x}$.

2 Methods

This experiment is performed using the *Leybold Experiment Kit 667 552* [Didb], including the *Measurement Adapter 666 205* for data acquisition and an integrated superconductor measuring module. The measuring module consists of a piece of $YBa_2Cu_3O_{7-x}$ superconductor and a Platinum-Irdium resistor as a temperature sensor, all encased within a metal mantle. The integrated measuring module can be plugged into the measuring adapter when required. $YBa_2Cu_3O_{7-x}$ is a high-temperature superconductor with an expected critical temperature around -180 °C [Didb]. The outputs of the adapter (voltage U_{temp} of the temperature sensor and voltage U_{sample} across the sample) are fed into the *Leybold Cassy 2 524 013* sensor module, which can be read out via the *Cassy 2* application on a computer. The two *Leybold* devices and their setup for measurements with the superconductor are depicted in fig. 1. A picture of the full setup can be found in fig. 13.

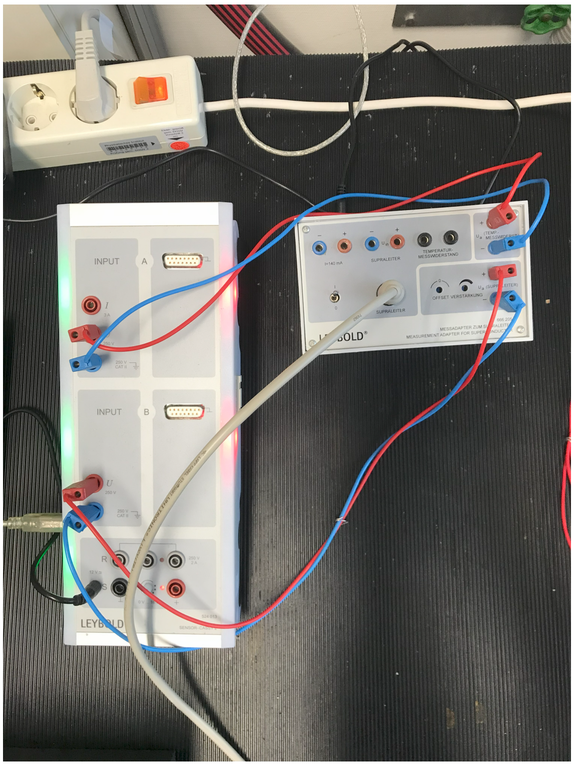

Figure 1: Measuring Adapter on the right and Cassy 2 Sensor on the left in the setting used for the measurements with the superconductor probe. The thicker grey cable plugged into the measuring adapter is connected to the superconductor probe head.

For the measurements with copper, a sensor head had to be built first. This was done by removing the isolation sheath from a piece of copper wire and soldering it onto a circuit board together with 4 contact wires. The length of copper wire between the outer most contacts is around $l = 11.6$ cm. The diameter of the wire is very thin and unknown to us, which is why we will not be able to take into account the samples geometry and calculate the resistivity from the measured resistance. The resistance of a conductor through which a current I is flowing and at which a voltage U can be measured is given by Ohm‘s law:

$$R = \frac{U}{I}. \tag{1}$$

As the current is in first approximation constant in our experiment, we will limit ourselves to examining the voltage U_{sample} across the sample as a function of temperature, which is then proportional to the resistance.

A Platinum temperature sensor of the model *Pt100* [BLA] is glued onto the copper wire and two wires are attached to it. A picture of the Cu measuring head can be found in fig. 2.

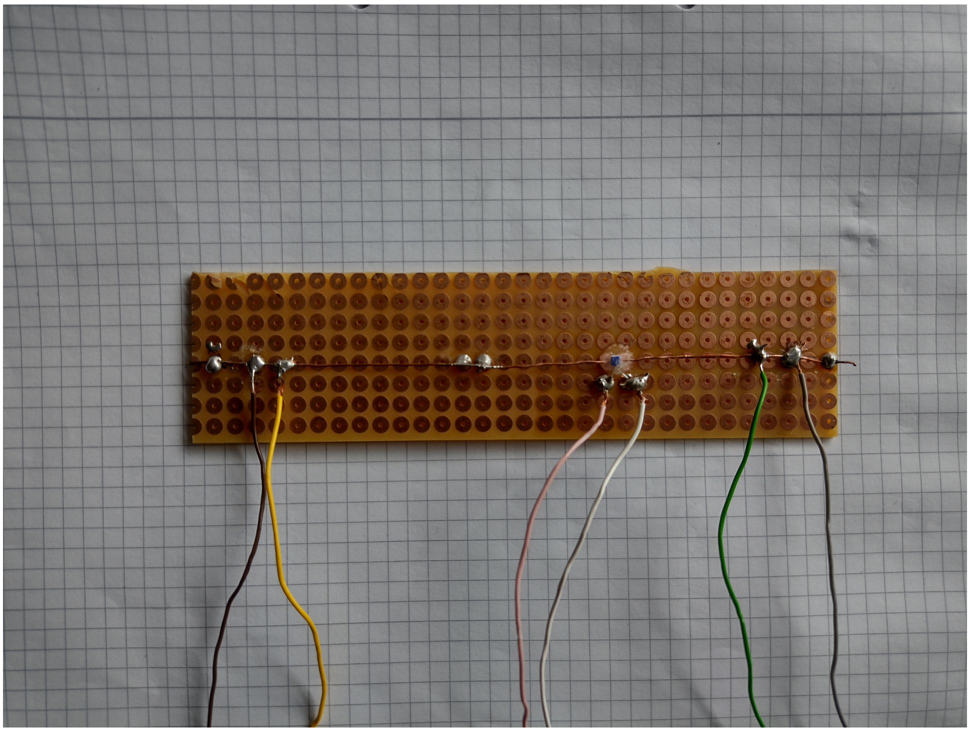

Figure 2: Measuring head with a piece of copper wire, contact cables for a 4-point-probe resistance measurement and a Platinum temperature sensor with wires.

For the measurements with the Cu sample, the two outer contacts on the copper wire are connected with the power output of the measuring adapter and the two inner contacts with the voltage input channels. This setup allows for a 4-point-probe measurement of the resistance of the sample, which is a technique that is used to avoid contact voltage losses and which allows for precise measurement of even very low resistance [al15]. The two contacts of the Platinum temperature sensor are connected to the respective black ports on the measuring adapter.

Additionally, an *EXTECH* multimeter [Ins] is used for measurements of the output current of the measuring adapter and the room temperature, the latter of which is done via a plug-in temperature measuring head. A Dewar flask and a plastic bucket with water complete the collection of necessary equipment. A supply of liquid nitrogen is hold at the ready.

In the data acquisition software, the voltages U_{temp} from the temperature sensor, and U_{sample} measured across the sample are recorded as a function of time. There are various settings to be chosen, like the range of the displayed voltage and the time intervals over which the program is averaging the recorded values. The integration time was kept at 200 ms during the whole experiment. Based on the respective peak voltages, the voltage range was set to (-0.3,0.3) V for the temperature sensor's output and (-1,1) V for the sample voltage.

Before measurements with the superconductor- and Cu samples are taken, the temperature sensors are calibrated, in order to be able to convert the voltage U_{temp} into a temperature T. This is done performing three different calibration measurements for each of the two probes. As a first reference, the room temperature is measured using the multimeter and the temperature probe which is placed close to the platinum sensor on the probe heads. A picture of this setup is shown in fig. 3 (a). After the voltage $U_{\text{room temp}}$ displayed by the data acquisition software was verified to be approximately constant over time - confirming that the probe had reached room temperature even if it had been cooled down before -, the momentary value was noted down.

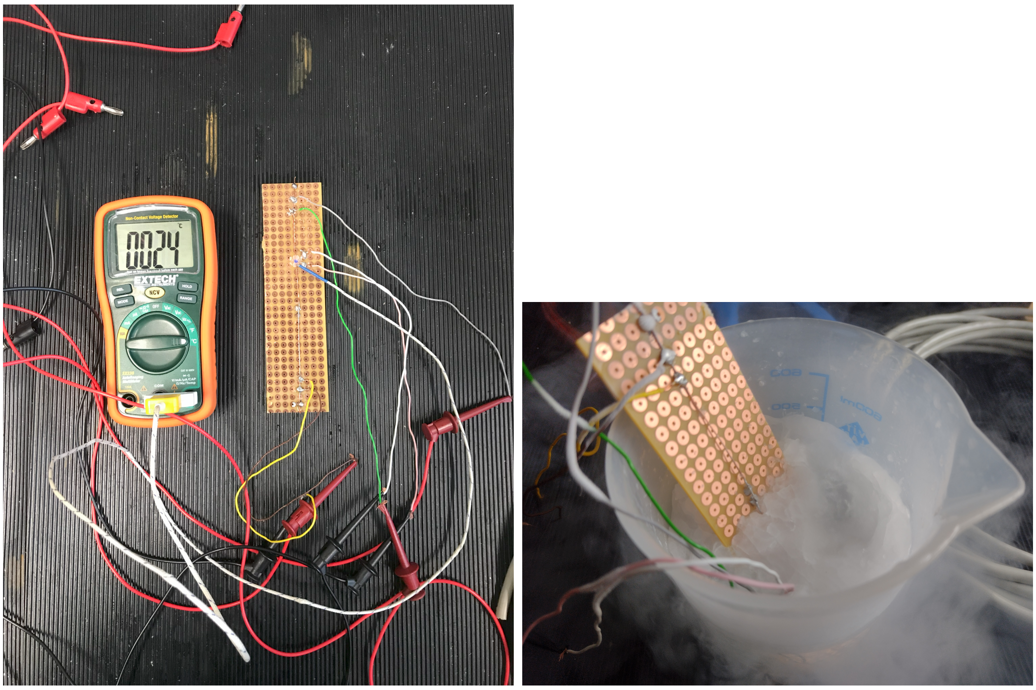

(a) Room temperature (b) Melting temperature of ice

Figure 3: Calibration measurements using (a) the room temperature and (b) the temperature at which ice melts for the Cu probe.

As a second reference for the calibration, we use the temperature at which ice melts, i.e. 0 °C. The probe is placed in a plastic bucket, which is filled with water, as can be seen in fig. 3(b). The water is brought to freeze by adding liquid nitrogen and the voltage U_{temp} is observed. After the ice is formed and the nitrogen has vaporised, a continuous decrease in voltage begins, corresponding to a rising temperature. When the melting point is reached, the temperature stays much longer at a steady value, due to the extra amount of energy required for the phase transition, before it continues to further increase. The corresponding plateau voltage is taken as the reference value $U_{\text{ice temp}}$.
Thirdly, the known boiling point of liquid nitrogen is used as an additional point for the temperature calibration. This is done by immersing the probes into the Dewar flask filled with liquid nitrogen and observing both the boiling behaviour of the nitrogen and the exponential temperature decay (voltage increase) on the screen. The maximum value of the voltage (minimum temperature) at which boiling is observed is recorded for both the superconductor and the Cu probe.

After the calibration measurements are complete, the stability of the output current is investigated by connecting the multimeter in the function of an amperemeter to the ports and observing the behaviour of the measured current over the course of a few minutes. The observations are discussed in section 3.2.

For the actual measurements of the temperature dependence of the resistance of the two discussed materials, the Dewar flask is filled again with liquid nitrogen and each of the probes is immersed into it, while the curves of temperature and voltage are recorded. After 2 to 5 minutes, the probes are removed from the flask and the heating process is recorded as well. This procedure is repeated several times, in order to assess the repeatability and gain more data for statistical significance.

3 Analysis and Results

Based on the measured data, we will first calibrate the temperature sensors, so that we can then examine the voltage at the two samples as a function of the temperature. The voltage data for the calibration were simply read off from the *Cassy* software display like described in section 2. The data from the other parts of the experiment were exported from the software and imported into Python for the analysis. These raw data are plotted in Appendix B, figs. 14 and 16 for reference.

The uncertainty on the measured voltages is given by the manual [Dida] as:

$$\sigma_{U,\text{syst}} = \pm 1\% \cdot U \pm 0.5\% \cdot U_{\text{range}}, \tag{2}$$

where the range end value U_{range} was, in our case, 0.3 V for the temperature sensor and 1 V for the sample voltages. We make the assumption that this uncertainty $\sigma_{U,\text{syst}}$ is a systematic error, while an additional statistical uncertainty comes from the limited resolution of the displayed values:

$$r = 0.0001\,\text{V for the displayed momentary values, used for the calibration,} \tag{3}$$

$$r = 0.00005\,\text{V for the values listed in the exported files (range } \pm 0.3\,\text{V),} \tag{4}$$

$$r = 0.0005\,\text{V for the values listed in the exported files (range } \pm 1\,\text{V).} \tag{5}$$

From these resolution widths r, we calculate the statistical uncertainty as for a rectangular distribution:

$$\sigma_{U,\text{stat}} = \frac{r}{2\sqrt{3}}. \tag{6}$$

3.1 Analysis: Calibration of the Temperature Sensors

Based on the information given in the manuals [Didb; BLA], we can, as an approximation, assume a linear relation between temperature and the output voltage from the temperature sensors. We therefore use the three temperature measurements that were performed for both of the sensors (at room temperature, ice bath and boiling nitrogen) in a linear calibration fit

$$U_{\text{temp}} = aT + b.$$

These fits are performed via orthogonal distance regression with the Python-module *scipy.odr* [com24] and take into account the statistical uncertainties on both temperature and sensor voltage.

For the statistical voltage uncertainties, we use the calculation from eqs. (3) and (6). On the reference temperatures, we estimate the following uncertainties:

For the room temperature (23 °C resp. 21 °C for the two calibration measurements), a statistical uncertainty component is given by the resolution of the display, assuming a rectangular probability distribution:

$$\sigma_{T_{\text{room}},\text{stat}} = \frac{0.05}{\sqrt{3}}\,{}^\circ\text{C}.$$

Additionally, there is a systematic uncertainty component on this value, stemming from the accuracy of the multimeter as listed in [Ins]:

$$\sigma_{T_{\text{room}},\text{sys}} = \pm 1\,\% \cdot T_{\text{room}} \pm 2.5\,{}^\circ\text{C}.$$

In order to simplify the following calculations, we add those three components for the room temperature quadratically:

$$\sigma_{T_{\text{room}}} = \sqrt{\left(\frac{0.05}{\sqrt{3}}\,{}^\circ\text{C}\right)^2 + (1\,\% \cdot T_{\text{room}})^2 + (2.5\,{}^\circ\text{C})^2}.$$

For the melting point of ice at $T_0 = 0\,{}^\circ\text{C}$, we estimate a statistical uncertainty of $\sigma_{T_0} = 0.5\,{}^\circ\text{C}$, due to the fact that we might not have hit the exact melting point from our observations of the plateau in the voltage U_{temp}:

$$T_0 = 0.0(5)\,{}^\circ\text{C}.$$

As a literature value for the boiling point of nitrogen, we find $T_{\text{boil, lit}} = 77.15\,\text{K} = -196\,{}^\circ\text{C}$ [Zha11]. During the calibration measurement, we observed the surface of the liquid nitrogen boiling. As there is most certainly a bit of a temperature gradient within the depth of the liquid, we assume a systematic deviation to lower temperatures and an according uncertainty on the calibration value and take

$$T_{\text{Nitr}} = -197.5(1.5)\,{}^\circ\text{C}$$

as our reference value for the calibration.

The resulting linear fits are shown in fig. 4. As a measure of goodness of the fits, we use the reduced χ^2, which is quoted in the respective plot legends.

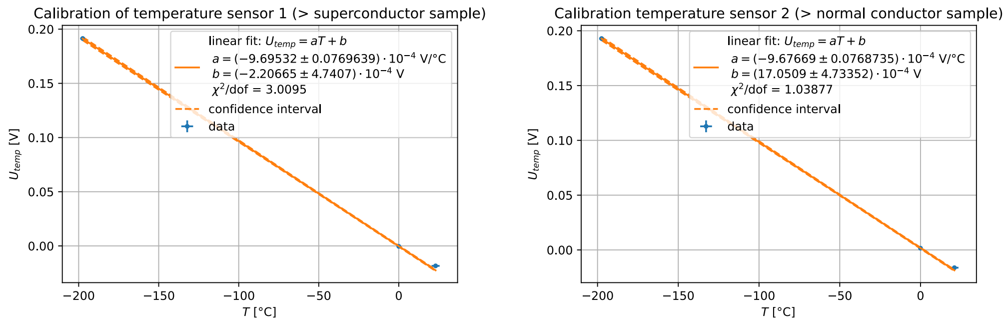

(a) First temperature sensor, used with the superconductor sample.

(b) Second temperature sensor, used with the normal conductor sample.

Figure 4: Calibration lines for the two temperature sensors.

The statistical uncertainties of the parameters a and b resulting from the fits are quoted in the legends of the plots in fig. 4. They are correlated with covariances of

$$\mathrm{cov}(a,b)_{\text{sensor 1}} = 1.1\,10^{-9} \cdot \frac{\mathrm{V}^2}{°\mathrm{C}}$$
$$\mathrm{cov}(a,b)_{\text{sensor 2}} = 1.1\,10^{-9} \cdot \frac{\mathrm{V}^2}{°\mathrm{C}}$$

(both corresponding to a correlation coefficient of 0.3). It is a coincidence that the rounded values are the same for both materials. Additionally, the systematic uncertainty on the voltage U_{temp} described in eq. (2) propagates into the fit parameter best values as

$$\sigma_{\text{a,syst}} = 0.1\,\% \cdot a \tag{7}$$
$$\sigma_{\text{b,syst}} = 0.5\,\% \cdot U_{\text{range}}. \tag{8}$$

As an overview, here are the parameter best values with both uncertainty contributions:

sensor 1:

$$a = -9.70\,(8)_{\text{stat}}\,(10)_{\text{syst}} \cdot 10^{-4}\,\mathrm{V/°C},$$
$$b = -2\,(5)_{\text{stat}}\,(15)_{\text{syst}} \cdot 10^{-4}\,\mathrm{V}.$$

sensor 2:

$$a = -9.70\,(8)_{\text{stat}}\,(10)_{\text{syst}} \cdot 10^{-4}\,\mathrm{V/°C},$$
$$b = 17\,(5)_{\text{stat}}\,(15)_{\text{syst}} \cdot 10^{-4}\,\mathrm{V}.$$

For the further analysis, we combine statistical and systematic uncertainties into total uncertainties on the calibration fit parameters:

$$\Sigma_{\text{a}} = \sqrt{\sigma^2_{\text{a,stat}} + \sigma^2_{\text{a, syst}}},$$
$$\Sigma_{\text{b}} = \sqrt{\sigma^2_{\text{b,stat}} + \sigma^2_{\text{b, syst}}},$$

From the voltages U_{temp} we can now calculate the corresponding temperatures T via:

$$T(U_{\text{temp}}) = \frac{U_{\text{temp}} - b}{a}. \tag{9}$$

We obtain a statistical uncertainty on T directly from the statistical uncertainty on U_{temp}:

$$\sigma_{\text{T, stat}} = \frac{1}{a}\sigma_{U_{\text{temp}},\text{stat}}. \tag{10}$$

The uncertainty contributions from the fit parameters, on the other hand, will have a common, directly correlated effect on all calculated temperatures (if the fit result for a is too large, for example, this will make all calculated temperatures too small). Therefore, we include these contributions into a systematic uncertainty $\sigma_{T,\text{syst}}$ together with the systematic uncertainty contribution from $\sigma_{U_\text{temp},\text{syst}}$:

$$\sigma_{\text{T, syst}} = \sqrt{\left(\frac{1}{a}\,\sigma_{U_\text{temp},\text{syst}}\right)^2 + \left(\frac{1}{a}\,\Sigma_\text{b}\right)^2 + \left(\frac{U_\text{temp} - b}{a^2}\,\Sigma_\text{a}\right)^2 + 2\,\text{cov}(a,b)\left|\frac{U_\text{temp} - b}{a^3}\right|}. \tag{11}$$

Any potential correlations between the uncertainty contributions except between $\sigma_{a,\text{stat}}$ and $\sigma_{b,\text{stat}}$ were neglected here, which will be discussed in section 4.1. The statistical component $\sigma_{T,\text{stat}}$ will later be taken into account when performing the fits on the temperature-voltage curves, while the $\sigma_{T,\text{syst}}$ will be applied to the fit results.

3.2 Analysis: Transition Temperature of $YBa_2Cu_3O_{7-x}$

Applying the above described calibration to the voltages U_temp, we can now examine the data for the voltage U_sample across the sample as a function of temperature. The measurement adapter should provide a nominal constant current of 140 mA, so that the resistance R_sample should be simply proportional to the measured voltage U_sample.

In order to assess how stable this current is in reality, we connected the power output sockets on the measurements adapter [Didb] with the multimeter and observed the resulting current before performing the actual cooling and heating measurements with the superconductor probe. The observation made was that there is a slow but steady increase in current over time, which is not influenced by factors like movement of the device or temperature. We observed an increase in current by approximately 0.3 mA within 5 min at a current of around 135 mA, thus corresponding to a 0.2 % increase every 5 min. As we allowed the probe to cool down in the liquid nitrogen for around 5 min and observed the heating process afterwards for another 5 min, we can expect a relative increase in current of around 0.4 % during this. In approximation, the same increase should also affect the voltage U_sample. We will come back later to this effect and for now, regard the voltage as an approximate measure for resistance.

In order to gain some statistical significance, we performed the cooling and heating process several times. From comparing the plotted data sets (Appendix B, fig. 15) we can see that there is a certain amount of fluctuation between them, which we would like to take into account as an additional statistical uncertainty component on $U_\text{sample}(T)$. We observe that the difference between curves from different measurements increases with increasing temperature. This can partially be explained by above described increase in current over time: as we started by cooling down the probe and heated it up again afterwards, there is an expected increase in current over time and the difference between the two curves will be largest for the start and end temperature, respectively, thus at the high temperature end of the plot. However, this effect (expected influence $\approx 0.4\,\%$ as noted above) is not big enough to completely explain the fluctuation between the curves from different measurements. We will discuss some other possible factors later in section 4.2. For now, we quantify the fluctuations by assuming them to increase approximately linear with increasing temperature, starting from the minimal reached temperature $T_\text{min} \approx -197\,°\text{C}$. By estimating the maximum fluctuation at highest temperature between the two first measurements ("Heating 1" and "Cooling 1") visually from the plotted data, we get:

$$\sigma_{U_\text{sample},\text{fluct}}(T) = (T - T_\text{min}) \cdot 10^{-4}\,\text{V}/°\text{C}.$$

This gives us an additional statistical component on the uncertainty on U_sample, which we combine with the statistical uncertainty $\sigma_{U,\text{stat}}$ stemming from the display accuracy of the software (eqs. (5) and (6)):

$$\sigma_{U_\text{sample},\text{stat}} = \sqrt{\sigma_{U,\text{stat}}^2 + \sigma_{U_\text{sample},\text{fluct}}^2}. \tag{12}$$

Having analysed the differences between the repeated measurement series and included this into the error calculations, we now decide on one single measurement series for a detailed analysis. Since the cooling process was happening faster than the heating process, the latter is supposed to be more reliable: First, a slower process allows more finely spaced data acquisition, and second, a faster process could introduce systematic errors if either the temperature sensor or the superconductor

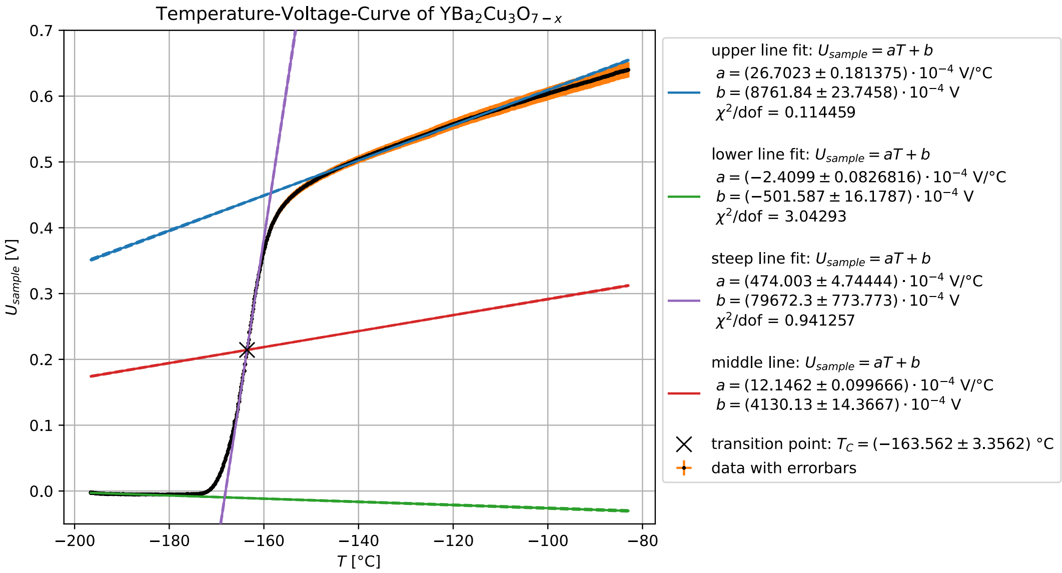

Figure 5: Sample voltage as a function of temperature for the superconductor $YBa_2Cu_3O_{7-x}$. Statistical uncertainties on the data are given by eqs. (10) and (12). Multiple linear fits are used to determine the transition temperature. Confidence intervals of the fits are too thin to be visible.

sample changes faster in temperature than the other one, resulting in a difference between the measured and the actual sample temperature. We thus decide to use the data from the first heating process in the further analysis. This is plotted in fig. 5.

As visible from fig. 5, the voltage drop does not happen abruptly once reaching the transition temperature, but with a certain slope. The transition temperature T_c is defined to be in the middle of this slope. We use the following procedure to obtain the value of T_c:

First, we fit straight lines to the linear areas of data, to the right and left of the voltage drop. The fits are again performed using orthogonal distance regression and the python module *scipy.odr* [com24] and a linear model of the shape

$$U_{\mathrm{sample}} = a\,T + b.$$

These fits are illustrated as the blue and green curves in fig. 5 and yield the best fit parameters $a_{\mathrm{upper}}, a_{\mathrm{lower}}, b_{\mathrm{upper}}$ and b_{lower}, the values and statistical uncertainties of which are given in the plot legend.

By taking the average values of both fit parameters, we obtain the parameters for a third straight line, which lies in the middle between the upper and lower fit (in red in fig. 5):

$$a_{\mathrm{middle}} = \frac{a_{\mathrm{upper}} - a_{\mathrm{lower}}}{2} \tag{13}$$

$$b_{\mathrm{middle}} = \frac{b_{\mathrm{upper}} - b_{\mathrm{lower}}}{2} \tag{14}$$

The corresponding uncertainties are propagated according to Gaussian error propagation. We assume total correlation, i.e. the correlation coefficient is

$$\mathrm{corr}(a_{\mathrm{middle}}, b_{\mathrm{middle}}) = 1,$$

since the values a_{upper} and b_{upper} are dominating here and their correlation coefficient - just like the lower line's correlation coefficient - is also approximately 1 (less than one percent deviation in both cases).

Finally, another linear fit is performed on the steep part of the voltage drop (purple line), resulting in a_{steep} and b_{steep}. The values and statistical uncertainties are again given in the legend.

Next, we use the intersection point between $U_{\mathrm{steep}}(T)$ and $U_{\mathrm{middle}}(T)$ to obtain T_c:

$$T_\mathrm{c} = \frac{b_\mathrm{middle} - b_\mathrm{steep}}{a_\mathrm{steep} - a_\mathrm{middle}} \tag{15}$$

with a statistical uncertainty resulting from the following error propagation:

$$\sigma_\mathrm{Tc,\ stat} = \sqrt{\left(\frac{1}{a_\mathrm{s} - a_\mathrm{m}}\,\sigma_\mathrm{bm}\right)^2 + \left(\frac{1}{a_\mathrm{s} - a_\mathrm{m}}\,\sigma_\mathrm{bs}\right)^2 + \left(-\frac{b_\mathrm{m} - b_\mathrm{s}}{(a_\mathrm{s} - a_\mathrm{m})^2}\,\sigma_\mathrm{am}\right)^2 + \left(\frac{b_\mathrm{m} - b_\mathrm{s}}{(a_\mathrm{s} - a_\mathrm{m})^2}\,\sigma_\mathrm{as}\right)^2 \\ +2\,\mathrm{cov}(a_\mathrm{m}, b_\mathrm{m})\left|-\frac{b_\mathrm{m} - b_\mathrm{s}}{(a_\mathrm{s} - a_\mathrm{m})^3}\right| + 2\,\mathrm{cov}(a_\mathrm{s}, b_\mathrm{s})\left|\frac{b_\mathrm{m} - b_\mathrm{s}}{(a_\mathrm{s} - a_\mathrm{m})^3}\right|},$$

where "s" labels the parameters of the steep fitted line and "m" the ones of the averaged middle line.

Until now, systematic uncertainties were neglected in this section. The systematic uncertainty on U_sample should only shift or stretch the whole plot in vertical direction, so that it has no effect on the calculated transition temperature. The systematic temperature uncertainty (eq. (11)), though, directly affects T_c. We therefore calculate the systematic uncertainty $\sigma_{T_c,\mathrm{syst}}$ by applying eq. (11) (where we replace $\frac{U_\mathrm{temp}-b}{a} = T_c$) to the calculated value of T_c. The two uncertainty components are then

$$\sigma_\mathrm{Tc,\ stat} = 3.4\,^\circ\mathrm{C}, \tag{16}$$
$$\sigma_\mathrm{Tc,\ syst} = 3.3\,^\circ\mathrm{C}. \tag{17}$$

They can be combined by quadratic addition into one total uncertainty on the end result:

$$T_\mathrm{c} = -164(5)\,^\circ\mathrm{C}. \tag{18}$$

3.3 Analysis: Temperature Dependence of the Resistance of Cu

Analogous measurements as for the superconductor sample were performed with the Cu sample. Again, the temperature values were calculated from the corresponding calibration in section 3.1, and the measurement uncertainty on the sample voltage was given by eqs. (5) and (6). The resulting temperature-voltage-curves from all measurement series are shown in fig. 6.

Notably, the curves acquired from the cooling processes vary among each other and deviate from a linear function more strongly than any of the heating curves. Their data are also a lot less densely spread over large temperature ranges. Both effects stem from the fact that the cooling process was happening significantly faster, and imply that the data from the heating processes are again more reliable. A detailed discussion of these effects follows in section 4.3. We will therefore focus on the three heating curves for now.

While the first and second heating process don't vary strongly from each other, the third one, which was conducted one day later, does deviate especially at low temperature. Potential reasons for this will also be discussed in section 4. For now, the same procedure as for the superconductor sample is applied: We estimate an additional statistical uncertainty based on the variation between different measurement series and then continue with a detailed analysis of only one of the curves. In contrast to the experiments with the superconductor, in this case here the variation between measurement series is largest at low temperatures. Due to that, we now use the ansatz of an uncertainty $\sigma_{U_\mathrm{sample},\mathrm{fluct}}$ that is proportional to the measured temperature. By estimation based on the plot, we decide on the specific values

$$\sigma_{U_\mathrm{sample},\mathrm{fluct}} = -T \cdot 10^{-5}\,\mathrm{V}/^\circ\mathrm{C}.$$

Like before, this is combined with the measurement uncertainty $\sigma_{U,\mathrm{stat}}$ eqs. (5) and (6) to a total statistical uncertainty of

$$\sigma_{U_\mathrm{sample},\mathrm{stat}} = \sqrt{\sigma^2_{U,\mathrm{stat}} + \sigma^2_{U_\mathrm{sample},\mathrm{fluct}}}. \tag{19}$$

With that, the first heating curve (blue in fig. 6) is chosen for a detailed analysis. Like the other two heating curves, it is approximately linear over most of the covered temperature range, but begins to decrease steeply around -190 °C. First, we perform a linear fit

$$U_\mathrm{sample} = aT + b$$

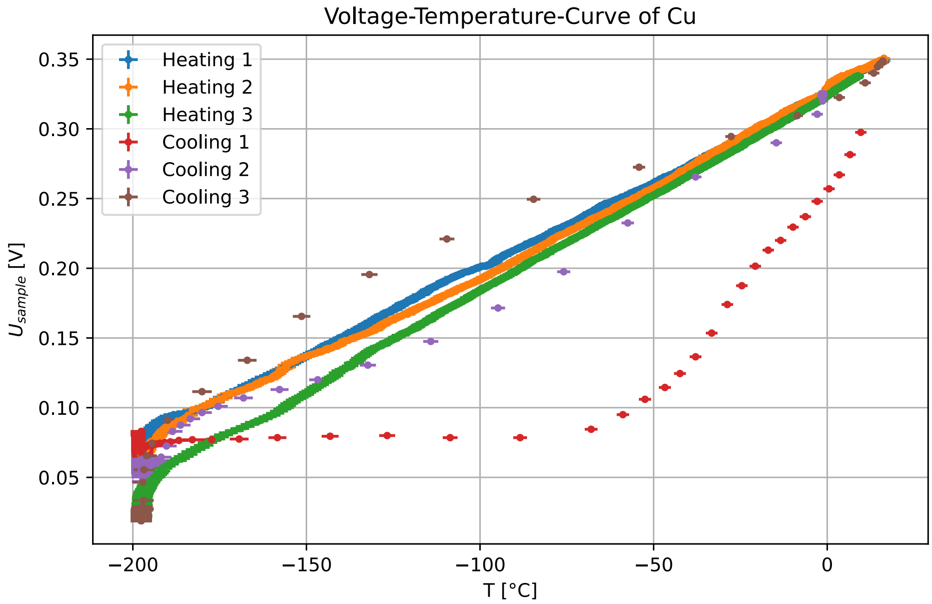

Figure 6: Sample voltage as a function of temperature for the normal conductor Cu in repeated measurement series. Statistical uncertainties on the data are given by eqs. (5), (6) and (10).

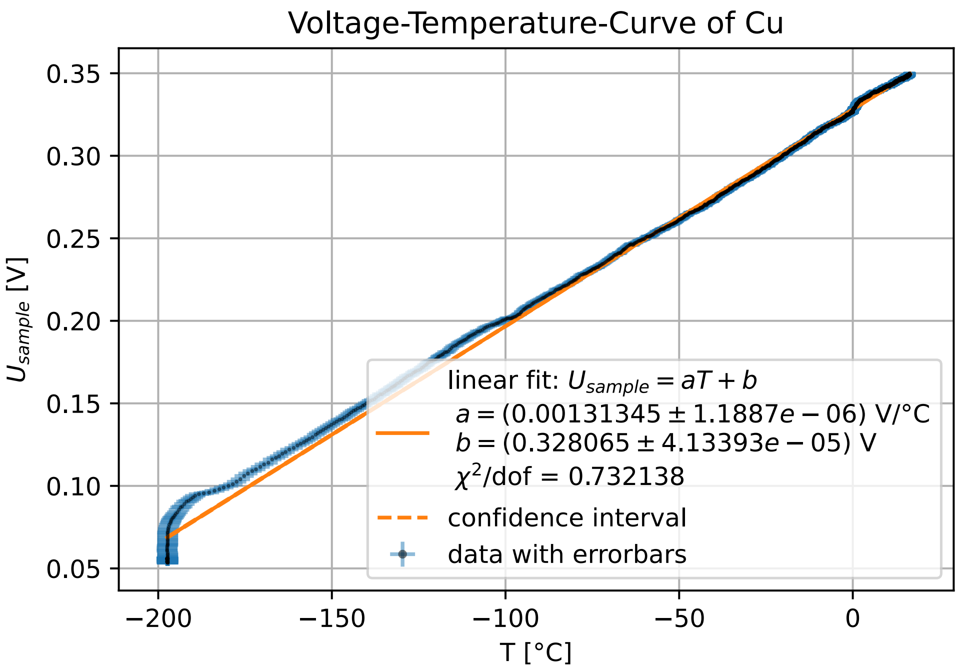

Figure 7: Sample voltage as a function of temperature for the normal conductor Cu in one selected measurement series (first heating process). Statistical uncertainties on the data are given by eqs. (10) and (19). This fit was performed using data from the whole temperature range.

on the whole temperature range which is shown in fig. 7. To quantify the deviation at low temperatures, we additionally perform a series of linear fits using only parts of the data, each in a different temperature interval: Keeping the interval's upper bound fixed at the maximal value, we vary the lower bound and investigate what influence that has on the fit. In fig. 8, the resulting reduced χ^2-values are plotted to give an impression of the fit quality dependence on the amount of data used in the fit. Additionally, for each of the parameters a and b, the mean from the various fits was calculated:

$$\begin{aligned} \hat{a} &= 0.001308\,(5)_{\text{stat}}\,(67)_{\text{syst}}\ \text{V}/{}^\circ\text{C}, \\ \hat{b} &= 0.32816\,(7)_{\text{stat}}\,(645)_{\text{syst}}\ \text{V}, \end{aligned} \tag{20}$$

where the systematic uncertainties are propagated from eqs. (2), (5) and (11). For each fit with results a and b, the relative deviations $\frac{\Delta a}{\hat{a}} = \frac{a-\hat{a}}{\hat{a}}$ and $\frac{\Delta b}{\hat{b}} = \frac{b-\hat{b}}{\hat{b}}$ from these mean values are plotted in fig. 8 as well, showing how strong the actual fit results depend on the chosen fit interval.

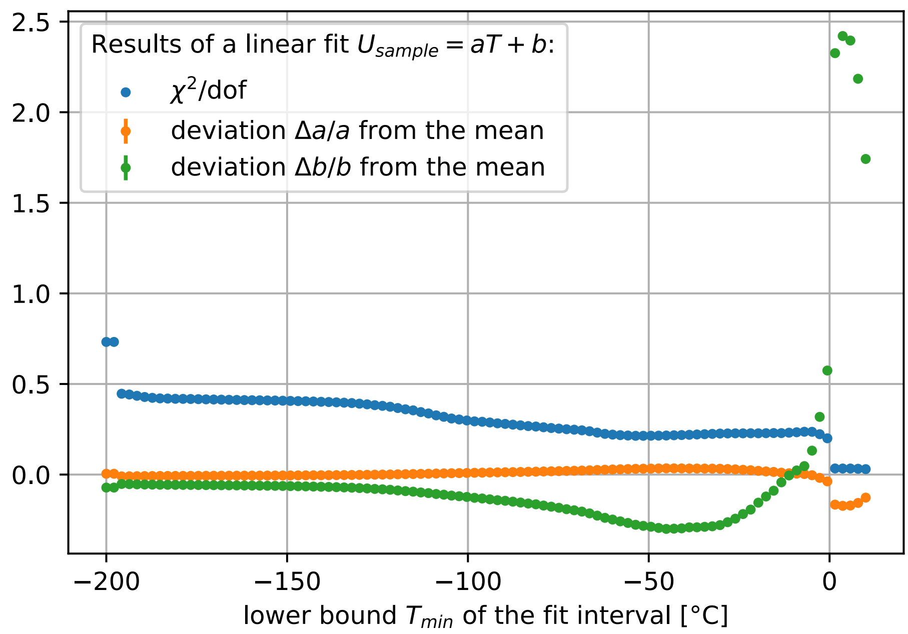

Figure 8: Results from linear fits like the one in fig. 7 for different fit intervals.

There are two points in the resulting plot where the fit results and quality change abruptly: One of them is at 0 °C, where an offset occurs that is also visible in fig. 7 and for the second heating curve in fig. 6. Of course, in the calculations leading to fig. 8, it has an especially heavy influence since there are only few data points included in the fits with $T_{\text{min}} \approx 0\,^\circ\text{C}$. The other main deviation at low temperature, which is found to be around -197.3 °C using this plot, has a lower influence on the fit results since the many data with $T > -197.3\,^\circ\text{C}$ dominate at that point. This deviation corresponds to the sudden voltage decrease already mentioned. Potential reasons for these two main deviations will be discussed in section 4.3.

Despite the obvious systematic deviations from the linear model, the reduced χ^2 values are definitely below the expected value of 1 in all fits. Usually, this could imply that the statistical uncertainties were estimated too large. However, in this case, the dominating uncertainty is the resolution uncertainty which was directly calculated from the resolution of the exported values (eqs. (5) and (6)), so that even without our roughly estimated additional uncertainty $\sigma_{U_{\text{sample}},\text{fluct}}$, the maximal value of χ^2/dof is found to be at 0.8.

4 Discussion

4.1 Discussion: Calibration of the Temperature Sensors

As the first part of the here presented experiment, measurements were performed which were used to calibrate the two temperature sensors. In both cases, three reference temperatures were chosen and a linear model was fitted to the data points. It is noteworthy how close the resulting fits are to each other: with the model $U_{\text{temp}} = aT + b$, the fits yield parameter best values of

$$\begin{aligned}
&\text{sensor 1:} \\
&\qquad a = -9.70\,(8)_{\text{stat}}\,(10)_{\text{syst}} \cdot 10^{-4}\,\text{V/°C}, \\
&\qquad b = -2\,(5)_{\text{stat}}\,(15)_{\text{syst}} \cdot 10^{-4}\,\text{V}. \\
&\text{sensor 2:} \\
&\qquad a = -9.70\,(8)_{\text{stat}}\,(10)_{\text{syst}} \cdot 10^{-4}\,\text{V/°C}, \\
&\qquad b = 17\,(5)_{\text{stat}}\,(15)_{\text{syst}} \cdot 10^{-4}\,\text{V}.
\end{aligned}$$

This speaks of the similarity between the two sensors, which are both Pt(-Ir)-sensors. Similar results were thus expected to a certain degree, though the closeness of the parameters a is still surprising. We can also have a look at the reduced χ^2 values in fig. 4 to assess how well the linear model describes our data with the estimated uncertainties:

$$\frac{\chi^2}{dof}_{\text{sensor 1}} \approx 3$$
$$\frac{\chi^2}{dof}_{\text{sensor 2}} \approx 1$$

As one can see, the quality of the fit is really good for the copper sample and slightly less good for the superconductor probe. There is of course the possibility that a model differing from the simple linear one would be better suited to accurately describe the calibration of the superconductor temperature sensor. With only three data points, however, it does not really make sense to fit more complex models. If one wanted to test the different fit functions, one would need a larger set of data.

For the here performed calibration we relied to a great extend on the known boiling point of nitrogen and the melting point of ice. The advantage of using these two reference values in comparison to more random temperatures (including the room temperature) is that one does not need to rely on the calibration quality of another device (the multimeter with plug-in temperature sensor in our case). In theory, those two data points alone would even be enough to define a linear calibration function.
On the downside, it was not at all trivial to identify the respective phase transitions correctly and especially in the case of the boiling temperature, a significant uncertainty stems from the fact that while the nitrogen at the surface had been boiling, the liquid some centimetres below the surface (where the temperature sensor was situated) might still have been cooler. This uncertainty might have been reduced by positioning the probe in a way that the temperature sensor would be directly at the surface of the boiling liquid. While this is a feasible idea for the self-build Cu-sensor for which the position of the Pt sensor is known, we do not know much about the positioning of the components within the integrated superconductor probe.

Additionally, it has to be noted that we did not actually deal with pure nitrogen and pure water respectively, as both substances were contaminated with each other from passing the probe back and forth. Having a mixture of two different substances could in general influence their boiling / melting point. As we do not know exactly how high the concentrations of contaminators were, it is difficult to make an estimation of how large this systematic effect might have been. Alternatively, one could have performed calibration measurements at varying temperatures using a well calibrated and precise thermometer.

Regarding the treatment of uncertainties during the calibration analysis section 3.1, quite a few assumptions and simplifications were made in order to keep the process comprehensible and avoid overly complicated calculations. One of those simplifications worth discussing is the treatment of the systematic uncertainty on the fit parameters a and b. This was first derived from a systematic uncertainty on the voltage U_{temp} eqs. (7) and (8) and later included in the error propagation for the systematic uncertainty on the temperature $\sigma_{\text{T, syst}}$ eq. (11). What was however not taken into

account is the fact that the systematic uncertainty components on a and b and the systematic uncertainty component of U_{temp}, which also appears in eq. (11), are actually correlated. Then again, the influence this would have on the total uncertainty is almost negligibly small.
On a similar note, we need to point out that we chose to combine systematic and statistical uncertainty components a few times in this report. It would in fact be cleaner to keep them separated for as long as possible, but it seemed more important to us to deliver a fairly concise and exemplary data treatment, rather than to include extremely lengthy error propagations taking into account all possible correlations.

4.2 Discussion: Transition Temperature of $YBa_2Cu_3O_{7-x}$

In the second part of the experiment, we determined the critical temperature of the superconductor $YBa_2Cu_3O_{7-x}$ by performing fits to the temperature-voltage curve of a heating process, after the probe had been cooled down to temperatures below T_c. The final result

$$T_c = -164(5)\,^\circ\mathrm{C} \tag{21}$$

lies a bit lower than the rough orientation value of $-180\,^\circ\mathrm{C}$ [Didb], but as the critical temperature depends on a lot of different factors, like the exact composition of the superconductor material, we cannot compare our result with any reference value. It does nevertheless seem to be a realistic value for such a high temperature superconductor and the uncertainty on our result is with $5\,^\circ\mathrm{c}$, corresponding to around 30% of the T_c, quite small considering the simple methods by which it was obtained.

One aspect that might hint at a kind of systematic error which we did not include in our analysis so far, is the fact that we observed such a strong fluctuation between different measurement series. While we are not able to fully explain these deviations, we can discuss a few possible contributing factors:
A first factor that was already brought up in section 3.2 is the drift over time that we observed in the current and which would impact U_{sample}. As already mentioned in the data analysis, we estimate that this effect to be at the largest $\approx 0.4\,\%$ between the beginning of one cooling and the end of one heating process. It has to be noted that we cannot say anything about the current flowing through the temperature sensor which is included in the superconductor probe head. This might be completely different from the current through the actual superconductor sample or might even show a drift of its own.
Secondly, we do not know much about in what geometry and how tightly the superconductor probe, the temperature sensor and the rest of the electronics are packed within their probe case. Depending on their orientation and the varying thermal capacities of the different materials, it seems likely that for example the superconductor might have heated up and cooled down faster than the Pt temperature sensor, leading to a systematic shift in the observed data. This is another factor that might have contributed to the curves of heating and cooling down processes being shifted with respect to each other.

We also need to address the point that while we did take into account the data sets from different measurements in order to estimate an additional statistical errorbar on them, we only chose one of the data sets to perform the rest of the analysis on, instead of combining the datasets. The problem here is that the data acquisition software recorded different amounts of data for different U_{temp}, depending on how fast the temperature change happened. Simply taking the average of two data sets is thus not possible. One, rather cumbersome, way of combining the data sets anyway might have been to divide them into small bins and use the average value within each bin as new data points, which could then be combined with data points from different measurements.
In the here presented analysis, we limited ourselves to including the fluctuations as an additional statistical uncertainty on U_{sample}. This was basically done via a visual estimation, from which we assumed the magnitude of fluctuation to be linearly increasing with increasing temperature. While this might have worked well as a first order approximation, the real nature of this statistical uncertainty component is not known, especially as we cannot fully account for it yet with the two explanations given above.

When looking at the treatment of statistical and systematic uncertainties in this part, one has to be aware of the fact that they are strongly influenced by the decisions made in section 3.1 and are mainly propagated through the various fits performed. For reasons of not wanting to over-complicate things, we included statistical uncertainty components in the fits and only brought up the systematic uncertainty on the temperature eq. (11) at the very end, as an additional uncertainty on the end result. Alternatively, one might have included this component already in the orthogonal distance regressions. As one can see from eq. (17), the systematic and statistic contributions on the final uncertainty are of the same order of magnitude.

As already mentioned before, one of the heating curves was chosen for the final analysis over one of the cooling curves, as it was suspected that the heating process, being much slower, would yield the more reliable data. One way of improving the experimental methods could be to come up with a way of having an even slower and more controlled change in temperature. We did experiment a bit with taking the probe out from and inserting into the liquid slower and faster, but this comes with difficulties of its own, as it might for example increase the risk for asymmetric temperature changes across the different probe head components, as described above as one possible systematic contribution to the drift observed between different measurement series.

Finally, it might have been interesting to take even more data, using multiple measurement series like we did, but with a more systematic method of varying possibly influential factors. For example, one could take repeated measurement series in an evenly spaced time series in order to identify the influence of the suspected temporal drift. Another idea would be to systematically vary the speed of the probe insertion into nitrogen, consciously producing an inhomogeneous heating. These kinds of measurements would allow to monitor the changes between different measurements in more detail, with the goal of a better quantification of potential systematic effects.

4.3 Discussion: Temperature Dependence of the Resistance of Cu

Also with the copper sample, the challenge of sensibly combining observations from different measurement series arose. Between the heating curves from day one of the experiment, no significant systematic deviation could be observed. The measurement taken on the following day, however, shows lower voltages especially at low temperature.

Possible reasons for these fluctuations are, as in the superconductor part, a varying current through the sample - though that would have a more important influence on the high temperature values -, a varying current through the temperature sensor - which would explain the linearly increasing deviation - or an inhomogeneous heating of the copper wire and the sensor. The latter effect is in particular a probable reason for the strong fluctuation between the cooling curves: Comparing the time evolution of the voltages in figs. 14 and 16 (Appendix B), it becomes evident that the cooling process of the Cu probe was by far the fastest temperature change encountered in our experiment. While in the other parts of the experiment, the change of temperature was happening over tens and hundreds of seconds, the Cu probe cooled down in only a few seconds. This means that the cooling was happening quasi instantaneous during the insertion of the sample into the liquid nitrogen, and that any asymmetry in the way of inserting it would have potentially distorted the results. This is well visible in the first measurement ("Cooling 1", red in fig. 6, top right in fig. 16), where the probe was inserted more slowly: Here, we hypothesise that due to its high thermal conductivity, the copper wire was quickly cooled down as a whole as soon as it was partially inserted into the liquid nitrogen, while the temperature sensor was still above, weakly thermally coupled to the wire, and thus showed higher temperatures than the actual wire temperature (steep slope on the right in fig. 6). Only when the sensor itself reached the liquid nitrogen, its temperature began to decrease more quickly, while the sample was already at minimum temperature so that U_{sample} was nearly constant (quasi horizontal line on the left in fig. 6).

A solution to this homogeneity problem would be to use a more compact probe. This, however, was opposed to the idea of using a long wire in order to get higher resistivity, higher voltages and thus lower relative uncertainties. To reconcile compactness and wire length, one idea discussed during the experiment is to use a coiled or serpentine sample wire. Besides, the fact that the sample was open in direct contact to the thermal environment - the temperature sensor was covered in glue - promotes inhomogeneous cooling. In comparison: the superconductor sample, which was enclosed in an aluminium casing together with the corresponding temperature sensor, was cooling and heating more slowly (compare figs. 14 and 16) and thus presumably more homogeneously.

Regarding the heating processes where this error source was less influential, it was found that the expected linear model works over a large temperature range. Solely based on the χ^2/dof-value of 0.7, one could even say that it is, within the limits of statistical uncertainties, compatible with the data over the whole measured temperature range. However, two temperatures were found where the data from several measurement series notably deviate from the linear model: around 0 °C and around -197 °C.

At both of those points, one can see a kink in the data plotted in fig. 7. At 0 °C, this is just a minor effect and afterwards the curve seems to follow a close to linear function again. For the lowest temperatures recorded in this experiment, the effect is more pronounced and one can first see a hint of a plateau, when moving towards lower temperatures, and then a short steep drop in voltage. We noticed that both of those anomalies occur at the temperatures, at which phase changes in the involved materials ought to take place: at 0 °C, this might have been caused by ice (adhering to the measurement head) melting and around -197 °C, the liquid nitrogen being at its boiling point could influence the voltage drop in the observed way. For example, if there was sublimated water vapour adhering to the temperature sensor, the melting at 0 °C would temporarily slow down the sensor's heating compared to the sample. Additionally, at the lowest recorded temperatures, we operate very close to the limit of the working range of the Pt temperature sensor (-200 °C), as given in [BLA], which might also be a cause for a deviation.

As expected, the copper wire does not exhibit a sudden drop in resistance within the considered temperature range, as the high-temperature superconductor did. The close to linear voltage decrease observed for decreasing temperatures agrees with our expectations. As suggested by [Hyp], a deviation from this linear trend and convergence to a residual resistance $\varrho_0 > 0$ would be expected for temperatures lower than around 60 K, which is beyond the scope of the here performed experiment and could therefore not be observed. The exact parameter values calculated in our fit are not comparable to any reference value since we do not know the exact diameter of the copper wire and it is thus impossible to calculate the actual resistivity. However, the ratio

$$\alpha = \frac{1}{\varrho(0\,°\mathrm{C})}\frac{\mathrm{d}\varrho(T)}{\mathrm{d}T} = \frac{1}{U(0\,°\mathrm{C})}\frac{\mathrm{d}U(T)}{\mathrm{d}T} = \frac{a}{b}$$

should be independent of geometry and current and can therefore be directly compared to a literature value: In [Dem17], this temperature coefficient is given as $\alpha \approx 0.004\,\mathrm{K}^{-1}$, which is indeed the same value that the mean fit values given in eq. (20) yield:

$$\frac{\hat{a}}{\hat{\bar{b}}} = 0.0040(2)\,°\mathrm{C}^{-1}.$$

Despite the observed systematic deviations and the various approximations made during the analysis, this result thus seems to be in good accordance with the expected resistivity behaviour.

5 Conclusion

In this experiment, the temperature-voltage curves of the superconductor $\mathrm{YBa_2Cu_3O_{7-x}}$ and the normal conductor copper have been analysed and compared. Initially, calibrations of the two temperature sensors were performed and a probe head for the Cu sample was assembled. The probe heads were cooled down to nearly -200 °C using liquid nitrogen and the changing voltages U_{sample} were measured through a 4-point-probe technique. From the heating and cooling curves for the superconductor sample, its critical temperature could be deduced performing a number of linear fits:

$$T_\mathrm{c} = -164(5)\,°\mathrm{C}.$$

The temperature-voltage behaviour of copper was found to be linear in good approximation for the considered temperature range, in accordance with our expectation.
Reasons for fluctuations between different measurement series, various sources of uncertainty and deviations from the expectation were discussed and some ideas for potential improvements of the experimental methods were suggested.

References

[al15] I Miccoli et al. "The 100th anniversary of the four-point probe technique: the role of probe geometries in isotropic and anisotropic systems". In: *Journal of Physics: Condensed Matter* 27.22 (2015). DOI: 10.1088/0953-8984/27/22/223201. URL: https://iopscience.iop.org/article/10.1088/0953-8984/27/22/223201.

[AOA22] Bukola Babatunde Adetokun, Oghenewvogaga Oghorada, and Sufyan Ja'afar Abubakar. "Superconducting magnetic energy storage systems: Prospects and challenges for renewable energy applications". In: *Journal of Energy Storage* 55 (2022), p. 105663. ISSN: 2352-152X. DOI: https://doi.org/10.1016/j.est.2022.105663. URL: https://www.sciencedirect.com/science/article/pii/S2352152X22016516.

[BCS57] J. Bardeen, L. N. Cooper, and J. R. Schrieffer. "Theory of Superconductivity". In: *Phys. Rev.* 108 (5 1957), pp. 1175–1204. DOI: 10.1103/PhysRev.108.1175. URL: https://link.aps.org/doi/10.1103/PhysRev.108.1175.

[BLA] TESLA BLATNÁ. *Platinum temperature sensor PT100 data sheet*. URL: https://tesla-blatna.eu/downloads/Senzory/datasheet-Pt100.pdf.

[Bos24] Sarah Boslaugh. *Maglev*. Encyclopedia Britannica, accessed 25 september 2024. 2024. URL: https://www.britannica.com/technology/maglev-train.

[CER] CERN. *Pulling together: Superconducting electromagnets*. website accessed 25 september 24. URL: https://home.cern/science/engineering/pulling-together-superconducting-electromagnets.

[com24] The SciPy community. *Orthogonal distance regression*. Scipy.odr documentation, available online. 2024. URL: https://docs.scipy.org/doc/scipy/reference/odr.html.

[Dem17] Wolfgang Demtröder. *Experimentalphysik 2: Elektrizität und Optik*. 7th ed. Springer Spektrum Berlin, Heidelberg, 2017. DOI: https://doi.org/10.1007/978-3-662-55790-7.

[Dida] LD Didactic. *Cassy Lab 2 524 221en*. available as a PDF on Ilias. URL: https://ilias.uni-freiburg.de/ilias.php?baseClass=ilrepositorygui%5C&cmd=sendfile%5C&ref_id=3498859.

[Didb] LD Didactic. *Determining the transition tem- perature of a high-temperature superconductor*. available as a PDF on Ilias. URL: https://ilias.uni-freiburg.de/ilias.php?baseClass=ilrepositorygui%5C&cmd=sendfile%5C&ref_id=3498856.

[Hyp] The Physics Hypertextbook. *Condensed Matter*. available as a PDF on Ilias. URL: https://ilias.uni-freiburg.de/ilias.php?baseClass=ilrepositorygui&cmd=sendfile&ref_id=3498846.

[Ins] EXTECH Instruments. *Bedienungsanleitung True RMS Multimeter Modell EX530*. available as a PDF on Ilias. URL: https://ilias.uni-freiburg.de/ilias.php?baseClass=ilrepositorygui%5C&cmd=sendfile%5C&ref_id=3498855.

[MVG23] Marina Manso Jimeno, John Thomas Vaughan, and Sairam Geethanath. "Superconducting magnet designs and MRI accessibility: A review". In: *NMR in Biomedicine* 36.9 (2023), e4921. DOI: https://doi.org/10.1002/nbm.4921. URL: https://analyticalsciencejournals.onlinelibrary.wiley.com/doi/abs/10.1002/nbm.4921.

[Wer12] Reinhold Kleiner Werner Buckel. *Supraleitung*. John Wiley & Sons, Ltd, 2012. ISBN: 9783527668670. DOI: https://doi.org/10.1002/9783527668670. URL: https://onlinelibrary.wiley.com/doi/abs/10.1002/9783527668670.

[Zha11] Yiming Zhang. "Corrected Values for Boiling Points and Enthalpies of Vaporization of Elements in Handbooks". In: *Journal of Chemical & Engineering Data* 56 (2011). URL: https://pubs.acs.org/doi/full/10.1021/je1011086.

6 Appendix A: Signed Lab Notes

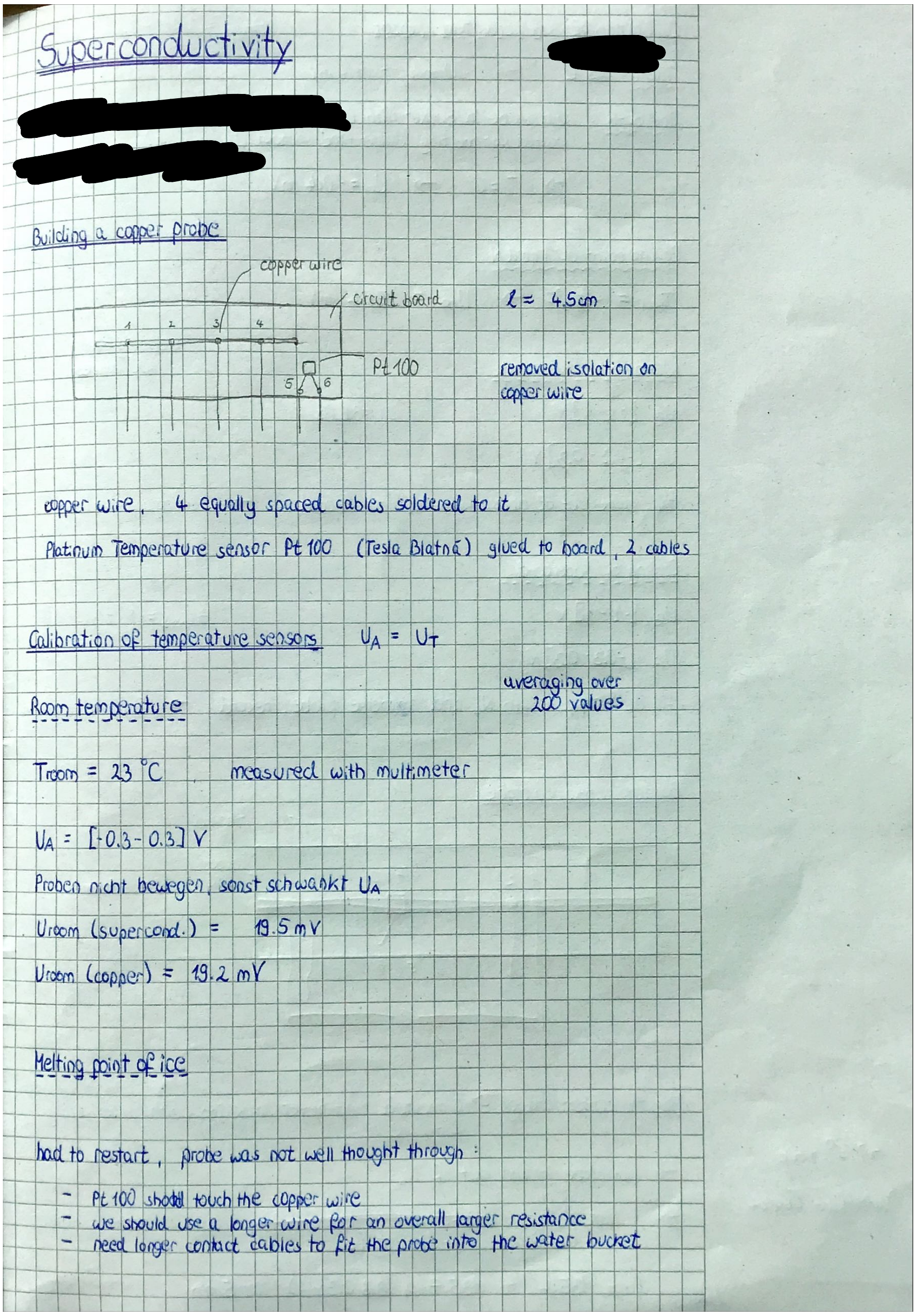

Superconductivity [redacted]

[redacted]

Building a copper probe

copper wire
circuit board
1 2 3 4
Pt 100
5 6

$l = 4.5\,cm$

removed isolation on copper wire

copper wire, 4 equally spaced cables soldered to it

Platinum Temperature sensor Pt 100 (Tesla Blatná) glued to board, 2 cables

Calibration of temperature sensors $U_A = U_T$

Room temperature

averaging over 200 values

$T_{room} = 23\,°C$ measured with multimeter

$U_A = [-0.3 - 0.3]\,V$

Proben nicht bewegen, sonst schwankt U_A

U_{room} (supercond.) = 19.5 mV

U_{room} (copper) = 19.2 mV

Melting point of ice

had to restart, probe was not well thought through:

- Pt 100 should touch the copper wire
- we should use a longer wire for an overall larger resistance
- need longer contact cables to fit the probe into the water bucket

Figure 9: Labnotes Page 1

Calibration of Supercond. temp sensor $\quad$ $\sigma_{T,sys} = \pm 1\% + 2.5°C$ (Multimeter)

$T_{room} = 23°C$ $\rightarrow$ $U_{room} = -18.4$ mV $\quad$ U_A [-0.3 - 0.3] V

Ice bath : put probe in bucket with water, added liquid N to freeze it, waited for melting (longer time without U_A changing)

$\rightarrow$ $T_0 = 0°$ $\rightarrow$ $U_0 = -0.4$ mV

$\sigma_{U_A,sys} = 1\% + 0.5\% \cdot 0.3V$

Boiling point of liquid N

$T_{boil} = -196°C$ $\rightarrow$ $U_{boil} = 191.4$ mV

averaging over 200 values

Warming of Supercond.

U_B [-1 - 1] V $\quad$ $\Delta t = 3000s$

U_A [-0.3 - 0.3] V

take probe out of dewar with N_L and record $\rightarrow$ „Heating Supercond.txt"

Cooling of Supercond.

U_B [-1 - 1] V $\quad$ $\sigma_{U_B,sys} = 1\% + 0.5\% \cdot 1V$

U_A [-0.3 - 0.3] V

fill dewar flask with N_L and immerse probe, record $\rightarrow$ „Cooling Supercond.txt"

Building a new Cu probe

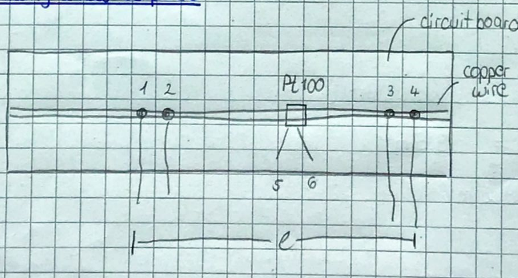

$l \approx 11.6$ cm

Does the current change? connected multimeter in series with power supply for wire

$\rightarrow$ put probe in and out of N_L

$\rightarrow$ I kept rising (~~134.9 mA - 135.6 mA~~), but no matter whether it was cooling down or heating up

from 135.4 to 135.7 mA (0.3 mA) in 5 min

27.09.2024

Wentao Chen

Figure 10: Labnotes Page 2

Calibration of Cu temp. sensor

Ice Bath : $T_0 = 0°C$ $U_0 = 1.4\,mV$ U_A [-0.3 - 0.3 V]

Boiling point liquid N : $T_{boil} = -196\,°C$ $U_{boil} = 192.8\,mV$

Room temp : T_{room} = 25 ~~24~~ °C U_{room} = ~~120.2~~ mV
24°C 115.2 mV

Statistical uncertainties

$T_{multimeter}$: ⊓ - distr. 2a = 1°C

U_A : ⊓ - distr 2a = 0.1 mV [-0.3 - 0.3]

U_B : ⊓ - distr 2a = 1 mV [-1 - 1]

T_0 negligible uncertainty

T_{boil} → look up reference value & uncertainty on it

Cooling of Copper

very fast → see data „Cooling Cu.txt"

Heating of Copper

observed strange kink in temperature curve → repeat measurement

„Heating Cu.txt" , „Heating Cu2.txt"

same effect. ideas : - phase change in water vapor ? Glue ?
- something non-linear in temperature sensor ?

Repeating Cooling & Heating for superconductor

! Something probably wrong with Cu Calibration data !

→ most probable problem with room temp. ? But different sensor shows similar result

→ repeat ice bath measurement ?

Figure 11: Labnotes Page 3

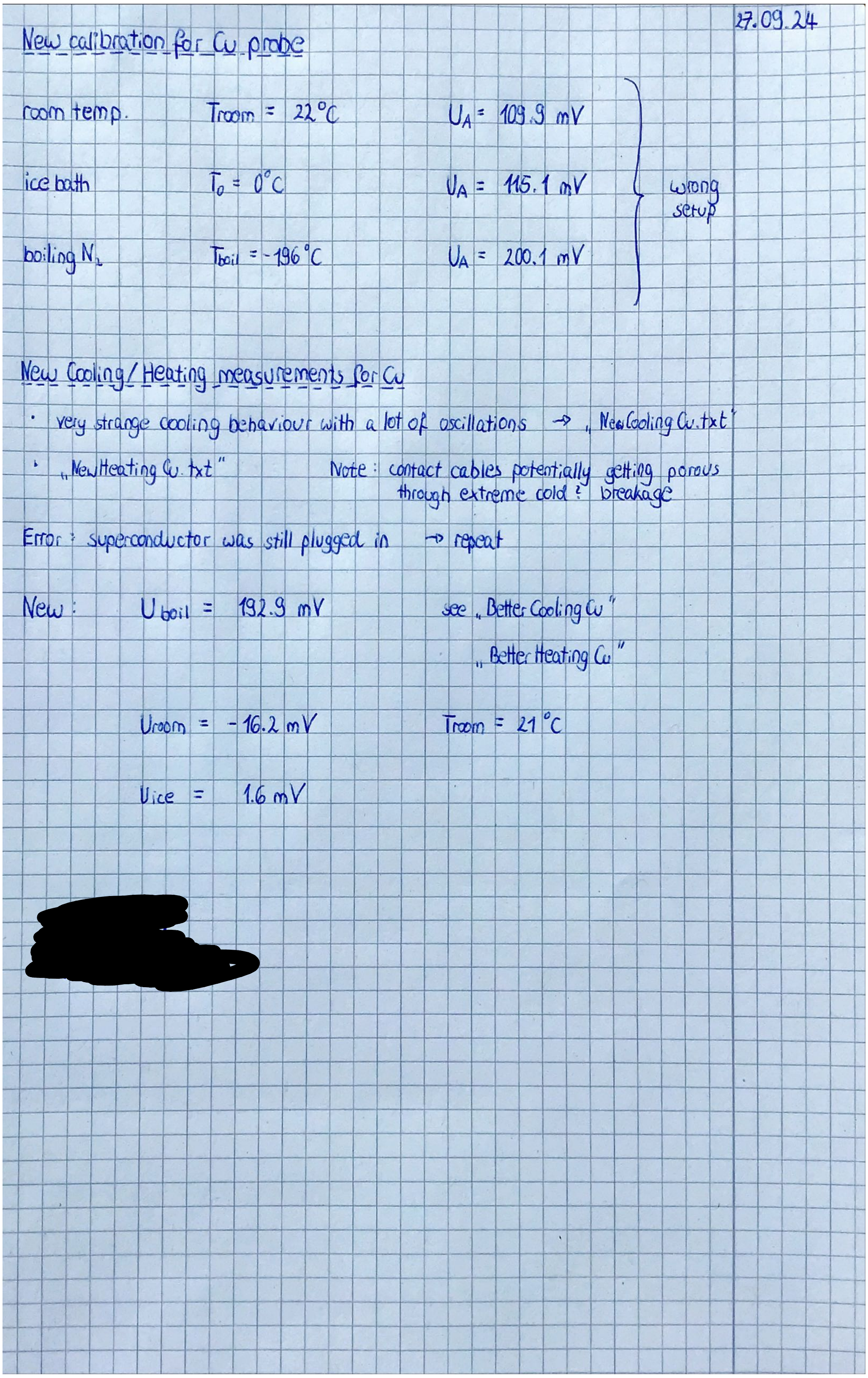
27.09.24

New calibration for Cu probe

room temp.	$T_{room} = 22\,°C$	$U_A = 109.9$ mV	wrong setup
ice bath	$T_0 = 0\,°C$	$U_A = 115.1$ mV	
boiling N_2	$T_{boil} = -196\,°C$	$U_A = 200.1$ mV	

New Cooling/Heating measurements for Cu

- very strange cooling behaviour with a lot of oscillations → „NewCooling Cu.txt"
- „NewHeating Cu.txt" Note: contact cables potentially getting porous through extreme cold? breakage

Error: superconductor was still plugged in → repeat

New: $U_{boil} = 192.9$ mV see „Better Cooling Cu" „Better Heating Cu"

$U_{room} = -16.2$ mV $T_{room} = 21\,°C$

$U_{ice} = 1.6$ mV

[redacted]

Figure 12: Labnotes Page 4

7 Appendix B: Additional Pictures and Data

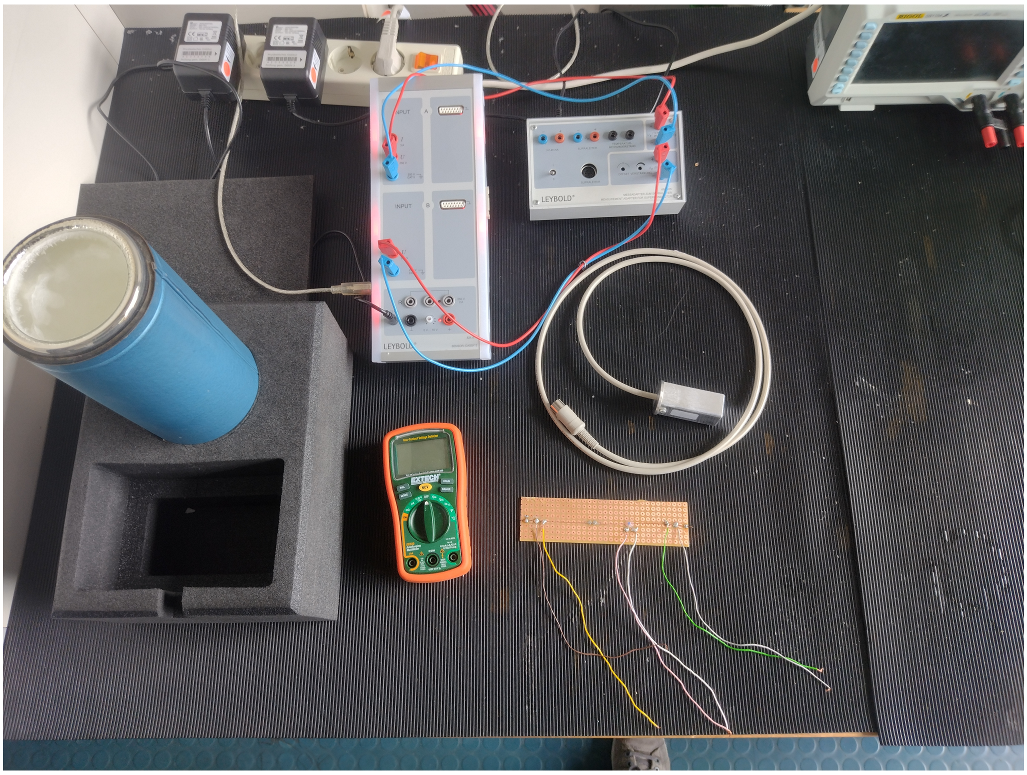

Figure 13: Picture of the full setup with (left to right, top to bottom): dewar flask, Cassy 2 sensor, multimeter, measuring adapter, superconductor probe, normal conductor probe.

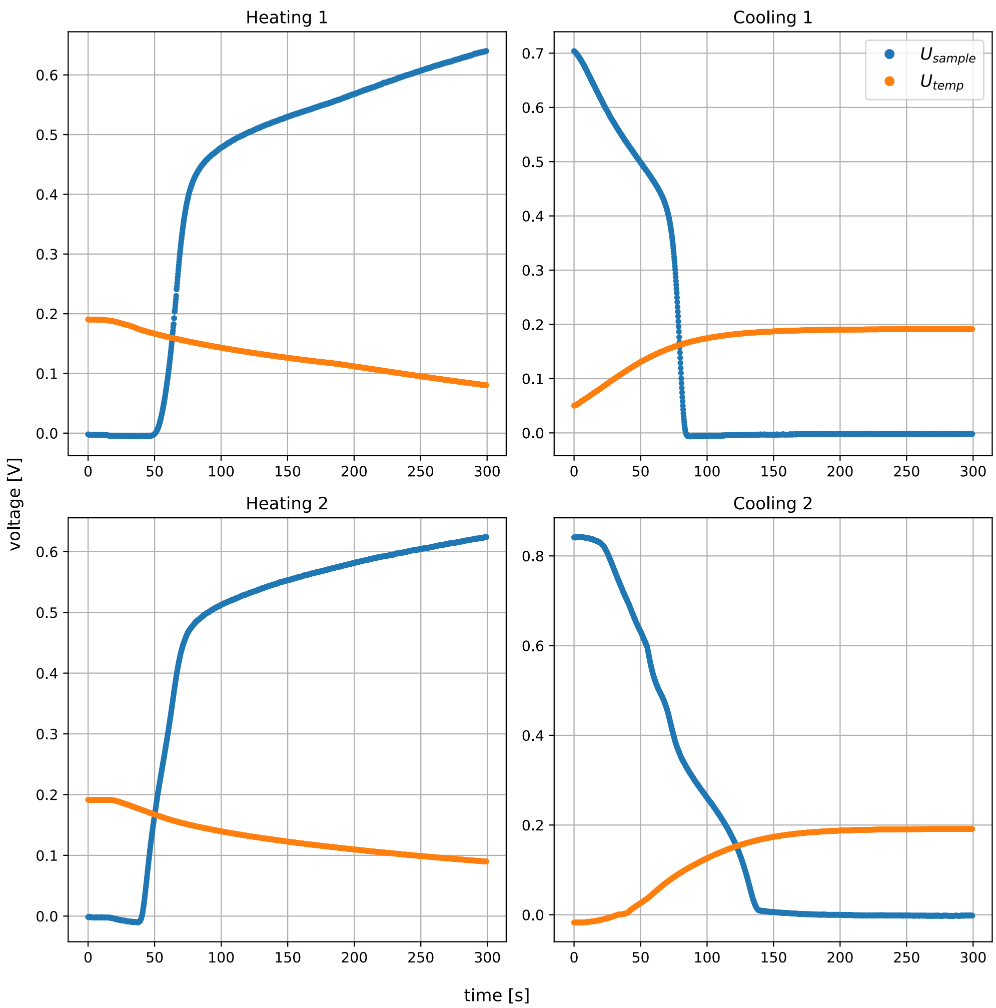

Figure 14: Raw data from the superconductor experiments.

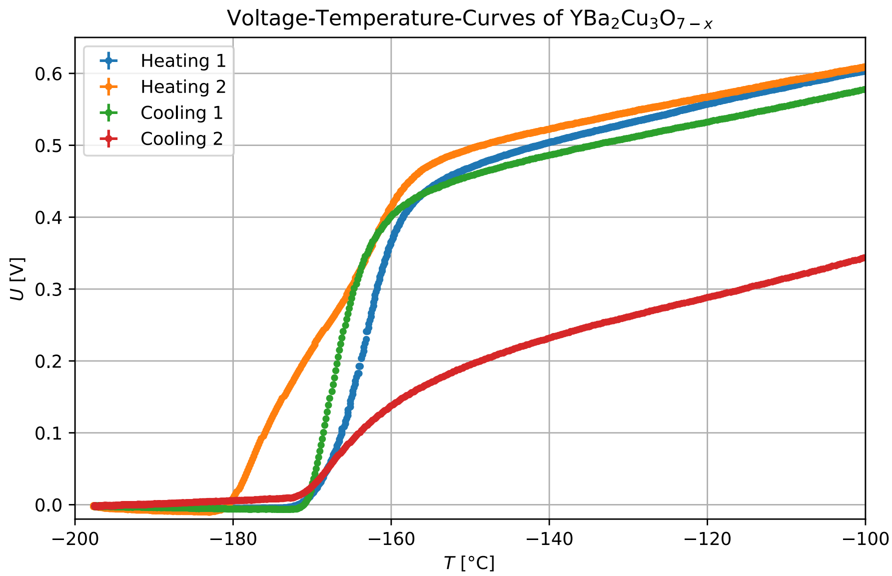

Figure 15: Voltage-temperature-curves for the superconductor sample from repeated measurement series. Statistical errors are given by eqs. (5), (6) and (10), but are too small to be visible in the plot.

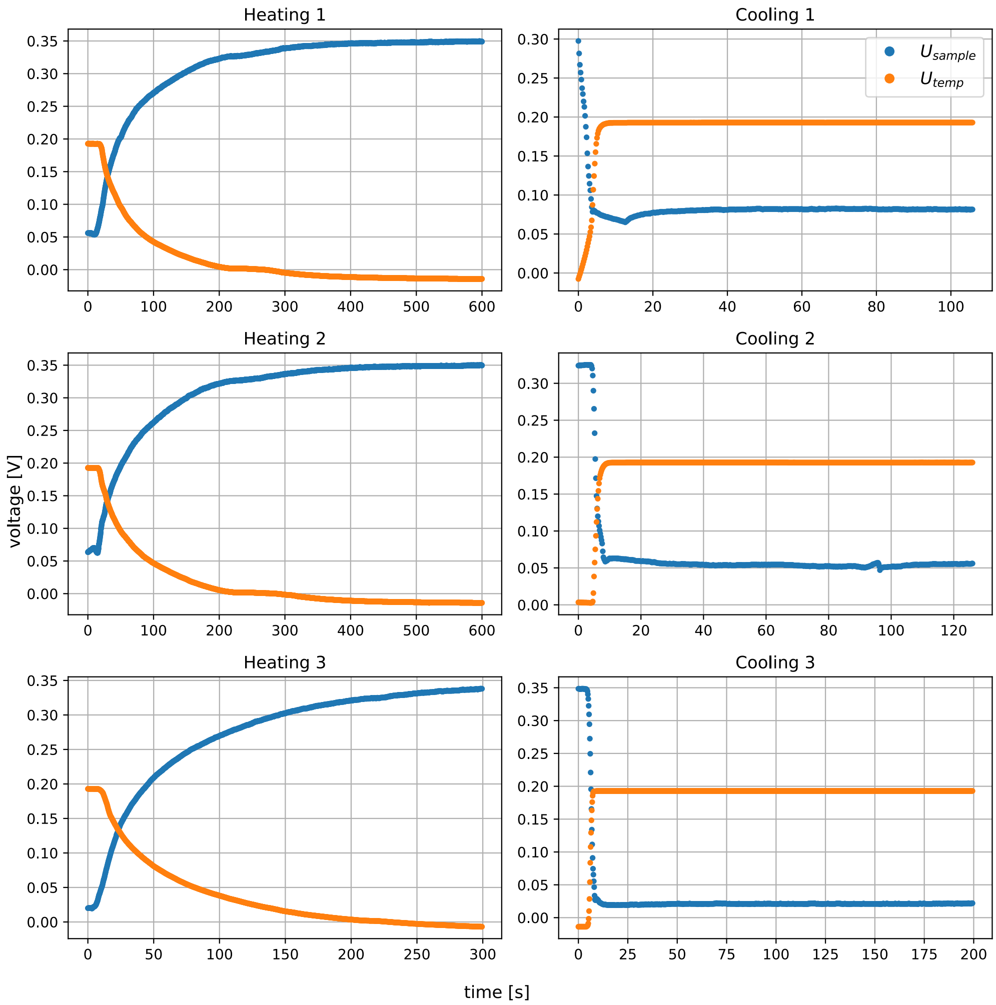

Figure 16: Raw data from the normal conductor experiments.